Porous Materials Prepared by Co-condensation Synthesis Approach

Ka-Lun Wong, Mohamad El Roz, Lubomira Tosheva, Jean-Michel Goupil, Svetlana Mintova, Mohamad El Roz

Porous Materials Prepared by Co-condensation Synthesis Approach

Ka-Lun Wong,[†] Mohamad El Roz,[†] Lubomira Tosheva,[‡] Jean-Michel Goupil,[†] and Svetlana Mintova[†,*]

*Corresponding author. E-mail: svetlana.mintova@ensicaen.fr

[†]Laboratoire Catalyse et Spectrochimie, ENSICAEN-Université de Caen-CNRS, 6 Bd. Maréchal Juin, 14050 Caen, France

[‡]School of Mechanical, Aerospace and Civil Engineering, The University of Manchester, Manchester M60 1QD, UK

Abstract

Porous silica materials were prepared by a single step co-condensation synthesis approach using 3-mercaptopropyltrimethoxysilane (MPTS) as organo-functional compound and silica co-source. For comparison, MPTS-modified amorphous silica and pure microporous (Silicalite-1) samples were synthesized. The incorporation of MPTS into the silica structures was confirmed by ^{29}Si and ^{13}C Nuclear Magnetic Resonance (NMR) and Raman spectroscopy, while the presence of two types of pores was verified with nitrogen sorption and X-ray diffraction (XRD) measurements of as-synthesized and calcined materials. The porous materials exhibited improved hydrophobicity in comparison with the samples prepared in the absence of MPTS. The presented method is simple and less toxic than the acid-meditated synthesis approach commonly applied for the preparation of hydrophobic zeolitic materials.

Introduction

Nanoporous materials with well-defined porous architecture are renowned for their traditional applications as catalysts, adsorbents and ion-exchangers [1-5]. Amongst them, the microporous (zeolites) and mesoporous molecular sieves (e.g. MCM- and SBA-type materials) are the two most intensively groups studied. The incorporation of organic moieties into their channels or anchored on their surfaces has provided them with distinctive properties

for a broad range of applications such as immobilization of enzymes, drug delivery carriers, encapsulation of metal nanoparticles, etc. [6-10].

Nanoporous materials can be functionalized by different pathways, which are categorized in two groups: (i) post-synthesis and (ii) direct synthesis approaches [11-12]. Post-synthesis methods involve treatment on the initially prepared porous materials, using grafting of organofunctional compounds onto the pore walls via covalent bonds [13]. The grafting process is a reaction between suitable organic moieties with the surface silanol groups of the material. The direct synthesis method involves co-condensation of an organofunctional compound with inorganic precursors during synthesis in a single step [13,14].

Ordered mesoporous materials have amorphous pore walls of hydrophilic nature. The large number of surface hydroxyl groups available can readily be utilized for post-synthesis grafting. A wide range of organic groups have been grafted on the pore walls of mesoporous silicas such as amine, phenyl, thiol, isocyanate and urea [15-19]. The post-synthesis grafting of microporous materials tends to change only the external surface due to their smaller pore sizes compared to the pore size of mesoporous silicas. In this case, post-synthesis grafting may lead to pore blocking. Thus, only few reports have been published on the modification of zeolites by grafting [20,21].

Alternatively, functionalization of the zeolite inner surfaces can be achieved by co-condensation method using organically-substituted trialkoxysilane reagents, [R'-Si$(OR)_3$], as a co-silica-source in addition to conventional silica sources. Pore blocking is not considered as a problem since the organic moieties become a part of the inorganic network structure. Instead of quaternary ammonium cations usually used as template in zeolite syntheses, various zeolite phases have been synthesized using quaternary ammonium-functionalized organo-siliconates such as N-trimethoxysilyl-propyl-tri-N-butyl-ammonium [22,23]. The zeolite phases were successfully crystallized by co-condensation method and it was demonstrated that the majority of the organosilicon Si-C bonds were cleaved in the as-synthesized zeolite, thus leaving only a small amount of alkylammonium moieties intact. Ryoo and co-workers have used similar ammonium-functionalized organosilanes, but with longer alkyl chains for the preparation of zeolitic materials possessing microporous/mesoporous hierarchical structures [24,25]. Recently, the preparation of zeolitic materials with hierarchical porosity by co-condensation using alkyl-triethoxysilane was also reported [26]. The nano-crystal size and mesoporosity of the materials were found to be dependent on the alkyl chain and the amount of alkyl-alkoxysilanes added into the synthesis

mixtures. Besides, the formation of hierarchical porosity in zeolitic materials by grafting of zeolite seeds with organosilanes larger than the micropore opening has been demonstrated [27,28]. The functionalization of the zeolite seeds perturb the zeolite crystal growth and hinder further agglomeration, which leads to the formation of secondary porosity in the mesopore range. For all materials, the hydrophobic-hydrophilic properties have not been studied in detail.

Organic-inorganic hybrid zeolite containing Si-CH_2-Si bridges has been successfully synthesized using methylene-bridged organosilane as a silicon source [29,30]. However, long bridging organic groups other than methylene are unlikely to be incorporated into the crystalline framework. Davis and co-workers reported on the synthesis of organic-functionalized molecular sieves (OFMSs) with shape-selective catalytic properties [31-34]. Pure silica zeolite Beta (BEA-type structure) in the presence of phenethyltrimethoxysilane and tetraethylammonium fluoride as structure-directing agent was also synthesized [33].

The aim of this work was to prepare porous materials by co-condensation method using 3-mercaptopropyltrimethoxysilane (MPTS) as template and silica source. Another objective was to prove the successful grafting and to evaluate the hydrophilicity/hydrophobicity of the functionalized MPTS porous sample compared to pure Silicalite-1 and amorphous silica.

Experimental

Preparation of porous samples

The amorphous colloidal silica (FD-SiO_2) (Aldrich, SM-30, 30 wt. % in water) was freshly freeze-dried prior use.

Silicalite-1 was synthesized from a precursor solution prepared from freeze-dried colloidal silica and tetrapropylammonium hydroxide (TPAOH, Alfa Aesar, 1 M in water) with a molar composition of 9 TPAOH: 25 SiO_2: 420 H_2O. The freeze-dried silica was first mixed with TPAOH and stirred overnight at room temperature. The clear suspension obtained was transferred to a PTFE-lined autoclave and left to crystallize in a conventional oven at 140°C for 48 hours. The obtained crystalline colloidal suspension was purified using a high speed centrifugation followed by re-dispersion in distilled water in an ultrasonic bath.

The MPTS-functionalized Silicalite-1 (MPTS-Silicalite-1) sample was prepared similarly, except that the silica sources used were FD-SiO_2 and MPTS (Alfa Aesar, 95 %). Typically, FD-SiO_2 was first mixed with TPAOH and stirred overnight at room temperature. MPTS was then added in the solution and stirred for additional 2 hours. The molar composition of the mixture was the same as above with 22.5 SiO_2 obtained from FD-SiO_2 and 2.5 SiO_2 added as MPTS. A clear purplish red (Burgundy) color solution was obtained and was subjected to crystallization at 140°C for 48 hours. The obtained crystalline suspension was recovered by filtration.

For the preparation of the MPTS functionalized silica (MPTS-SiO_2), the FD-SiO_2 was mixed with deionized water and stirred overnight at room temperature. After that, MPTS was added in the suspension (pH ~ 10) and stirred for additional 2 hours prior aging for 12 hours and heated at 140 °C for 48 hours. The suspension was filtrated and dried.

The removal of structure directing agent from as-synthesis samples has been performed by calcinations or by using a cold O_2-plasma treatement The calcination process of the sample is consisted of heating from RT to 500 °C with a heating rate of 1.75°/min, kept at 500 °C for 5 hours and then cooled down to room temperature in 5 hours. Cold O_2-plasma treatment has been performed at low pressure (350 Pa) without any temperature alteration as detailed in the reference [34].

Characterization methods

Powder X-ray diffraction (XRD) patterns of the samples were recorded using a STOE STADI-P diffractometer (Cu Kα, λ= 0.15406 nm), with 0.028 step size and 1s step time. Electron micrographs of the samples were recorded on a Philips XL30 FEG scanning electron microscope (SEM). The chemical composition of the as prepared samples was determined by X-ray Fluorescence (XRF) analysis with a MagiX PHILIPS PW2540. In addition the amount of carbon, nitrogen and sulfur were determined using a Thermoquest NA2500 automatic apparatus. Solid state CP-MAS NMR spectra of the samples were recorded on a Bruker MSL 300 spectrometer using a 7 mm probe, operating at 59.6 MHz for ^{29}Si and 75.5 MHz for ^{13}C, respectively. Deconvolution and fitting of the NMR spectra were performed using the Winfit program [36]. The Raman spectra were measured at room temperature with a Bruker Equinox 55 FT-IR spectrometer equipped with an FRA106/S FT-Raman module. For the nitrogen (N_2)

adsorption measurements, the powder samples were calcined at 550 °C and outgassed at 350 °C prior analysis with a Micromeritics ASAP 2420 surface area analyzer. Thermal (TG/TGA) analyses were performed using a Setaram TGDSC 111 analyzer (heating rate of 5 °C min^{-1}) in air.

The real-time in-situ FTIR spectroscopy studies of plasma treatment were performed on self-supporting wafers of zeolite MPTS-Silicalite 1 (~10 $mg.cm^{-2}$) placed in the plasma reactor, where a desired gas composition was sustained at low pressure (350 Pa) after evacuation under vacuum for several minutes. The dielectric barrier discharge was ignited with a 50 Hz sinusoidal power supply (2 kV) between two electrodes fused to the IR cell. During the experiments, the temperature increase due to the cold plasma process was below ΔT= 120 °C. The IR spectra were collected in transmission mode on a Bruker Vertex 80v equipped with a cryogenic MCT detector (4 cm^{-1} resolution, 8 scans, and acquisition time ~1.2 s). For a relative high amount of zeolite (>300 mg), the plasma treatment has been performed in an appropriate plasma reactor, without IR monitoring, and the treatment has been realised in the same condition wich cited above. The time of the treatment depend of the amount of zeolite, it is about 30 min for 300 mg.

The water mass gain rate upon exposure at constant temperature and relative humidity (RH) were used for a qualitative evaluation of the affinity of the pure silica and MPTS-modified samples towards water. The measurements were performed at 25 ºC using a CiSorp Water Sorption Analyzer (CI Electronics, UK). Calcined samples stored at ambient conditions were used in these measurements. The instrument allows two samples to be measured simultaneously. The samples were transferred from the vials to the instrument's chamber and the humidity was increased to 85%. The mass of the samples was recorded every 5-30 seconds over more than 5 hours.

Results and Discussion

General characterization

The crystalline nature of the Silicalite-1 and MPTS-Silicalite-1 samples was proven by X-ray diffraction (Fig. 1). Both samples exhibit diffraction patterns characteristic of the MFI-type crystalline phase. Besides, a mesoporous phase in the MPTS-Silicalite-1 sample is seen by the presence of a relatively broad diffraction peak at low 2θ (Fig. 1 b). The mesoporous peak at 1.8° 2θ is not present in the XRD pattern of the amorphous MPTS-SiO_2 and in the pure Silicalite-1 (Fig. 1). This can be explained by the co-condensation process occurring in the presence of MPTS as silica source and as template, leading to a high degree of framework cross-linking between the zeolite silica framework and the organosiloxane, thus resulting in the formation of both micro- and mesopores. In order to probe the porosity of these samples, calcination was carried out at 550 °C for 6 hours. No change in the crystallinity of the samples was measured however the mesoporosity was destroyed. Furthermore, the particle size and morphology in the calcined samples have not been changed.

In order to preserve the entire porosity of the MPTS-Silicalite-1 sample, a plasma treatment was carried out on this sample (see experimental section). Recently we have shown the efficiency of this process in the activation of microporous materials at relatively low temperature (<150 °C) [34]. This method could be useful for the thermally unstable materials. In our case, this technique has been used in order to preserve the mesoporosity of MPTS-Silicalite 1, unstable after calcinations at high temperature. As show Figure 2, all the Bragg peaks are preserved after removal of the templates under plasma. Figure 3 present the evolution of IR spectra of MPTS-Silicalite 1 during O_2-plasma treatment. A total disappearance of the C-H bands under plasma treatmentcould be observed after 10 min wich confirm the removing of the entire template and the liberation of zeolite porosity.

The morphological features of the samples revealed by SEM are shown in Figure 4. The Silicalite-1 consists of nanoparticles with almost spherical shape and a diameter of ca. 90 nm. The organo-functionalized sample, MPTS-Silicalite-1, contain nanoparticles with a size below 50 nm which tend to form larger agglomerates with an ultimate size between 200 and 1000 nm. In contrast to the crystalline appearance of MPTS-Silicalite-1 and Silicalite-1, the functionalized amorphous silica (MPTS-SiO_2) does not have any specific morphology and shape. The size and the shape of the MPTS-SiO_2 fibers are determined by the conditions of drying.

Incorporation of MPTS in silica samples

The incorporation of MPTS in the samples was proven by analyzing the sulfur content, and the data are presented in Table 1 as amount of element per 1g of SiO_2. In the as synthesized MPTS-SiO_2 sample about 1.9 mmol MPTS is present, while in the MPTS-Silicalite-1 retained 4.1 mmol MPTS per gram silica. Only 0.9 mmol TPAOH was occluded in the MPTS-Silicalite-1, which is the same as in Silicalite-1 material.

The incorporation of MPTS in the samples was confirmed by both ^{29}Si and ^{13}C CP-MAS NMR spectra (Figures 5 and 6). The ^{29}Si solid state NMR spectra of MPTS-Silicalite-1 and Silicalite-1 contain a main peak at -112 ppm and a weak peak at -102 ppm, which are attributed to Q^4 [$Si(OSi)_4$] and Q^3 [$Si(OSi)_3OH$] species, respectively [37,38]. Despite that the cross-polarizing technique is not quantitative, the intensity of the Q^4 peak is significantly higher than that of Q^3, meaning that only a small amount of defect sites (Si-OH) were formed in the both samples. In addition, two well-resolved peaks at -68 and -55 ppm were found for the organo-functionalized sample (MPTS-Silicalite-1, Fig. 5b). These peaks are attributed to T^3 [R-C-Si-$(OSi)_3$] and T^2 [R-C-Si$(OSi)_2OH$] species, respectively. The T^2 and T^3 species confirm the presence of organosilane centers from the MPTS, and show that the Si–C bonds remain intact during the synthesis. This is an indication for the high degree of framework cross-linking between zeolite silica framework and the organosiloxane from the MPTS.

To identify the organic moieties attached to the zeolite framework, the solid state ^{13}C CP-MAS NMR measurements were carried out on the three samples. The resonance peaks at 62.7, 16.3, 11.3 and 10.1 ppm in the spectrum of pure Silicalite-1 can be attributed to the ^{13}C sites originated from the structure directing agent TPAOH (Figure 6 a) [39-40]. Additional peaks positioned at 35.5, 34.7, 14.0 and 13.0 ppm were only observed in the MPTS-Silicalite-1 sample. The most prominent peaks from the mercaptopropyl group at ~35 and 23.8 ppm are present. According to previous studies, peaks at 37-38 ppm are observed for organo-functionalized mesoporous silica prepared in alkaline solution, when quaternary ammonium compounds as structure directing agent and MPTS as organo-functional compound were used [41-43]. These peaks are tentatively assigned to the carbon closest to the S from disulfide group (RS-SR) or oxidized sulfur products. However, these peaks were not observed when samples were prepared in acidic medium or using neutral co-block polymers as structure directing agent [44-45]. In the case of the MPTS-SiO_2 sample prepared in the absence of TPAOH, only the resonance peaks at 28.1 and 13.0 ppm identical to mesoporous silica functionalized with MPTS by post-synthesis grafting approach are seen (Figure 6 c) [37]. This leads to the suggestion that the SH thiol groups in the MPTS-Silicalite-1 sample are in strong interactions with the quaternary ammonium ions (TPA^+) after deprotonation in the aqueous

base medium (Scheme 1). Therefore the resonance peaks at position 35.5 and 23.8 ppm could be due to C_1 and C_2 from S_2 species, which are interacting with TPA^+. The splitting of C_1 peak into a doublet (35.5 ppm and 34.7 ppm) could be due to the conformational effects of the propyl chains incorporated in the zeolite channels. The two unresolved peaks at 14.0 and 13.0 ppm can be assigned to C_3 resonance from both species (see Scheme 1).

The presence of the MPTS compound in the as-prepared MPTS-Silicalite-1 sample was further studied by the Raman spectroscopy. The spectra of Silicalite-1, MPTS-Silicalite-1 and MPTS-SiO_2 samples are shown in Figure 7. In addition to the bands at 760, 1050, 1110, 1320 (doublet) and 1430 cm^{-1}, observed for Silicalite-1, the spectrum of MPTS-Silicalite-1 contains numerous bands. The bands at 650 and 740 cm^{-1} are assigned to $\nu_{C\text{-}Si}$ and $\nu_{C\text{-}S}$ stretching mode of the MPTS compound [46-47]. The bands at 1259 (doublet), 1302, and 1413 cm^{-1} are attributed to the C-H bending mode of the propyl chain of MPTS. These bands are slightly shifted in the MPTS-SiO_2 sample in comparison with MPTS-Silicalite-1, thus proving that the MPTS is incorporated in the channels of the MPTS-Silicalite-1 sample. Raman spectroscopy is an excellent tool for detection of SH groups due to their relatively intensive Raman scattering, however, only a weak band at 2750 cm^{-1} which is due to the SH stretching mode is detected for the MPTS-Silicalite-1 sample (see the insert in Fig. 7), which is in a good agreement with the ^{13}C CP-MAS NMR results.

In summary, the NMR and Raman spectroscopies support the conclusion that TPAOH is present in the pores of Silicalite-1and MPTS-Silicalite-1 samples. In the case of MPTS-Silicalite-1, the TPAOH coexist with the organic moieties Si-R- , while the mercapto-propyl moieties are anchored to the surfaces of the MPTS-SiO_2 sample. These statements are also supported by the chemical analysis data (see Table 1).

Thermal analyses (TG/TGA) of the samples were performed in oxidative conditions (Figure 8). The total weight losses of MPTS-SiO_2, Silicalite-1 and MPTS-Silicalite-1 were 15.1, 15.5 and 26.4 wt. %, respectively (Table 2). The main weight loss near 300 °C is shifted to higher temperatures in the following order: MPTS-Silicalite-1 (310°C) < MPTS-SiO_2 (320°C) < Silicalite-1 (345°C). Only the Silicalite-1 sample exhibits defined weight loss below 250°C. It can be ascribed to desorption of firmly bound water in addition to desorption of loosely bound water.

In the case of MPTS-SiO_2 a small weight loss at 260 °C (1.5%) and a steep weight loss at 320 °C (5.5 %) were measured, followed by a broad weight loss (7 %) at 390 °C and 520 °C. According to the literature, [48-49] the weight loss at 320 °C arises from elution of sulfur-containing molecules resulting from anchored propanethiol decomposition. Then propylene is

evolved from the grafted alkyl chains, and dehydroxylation or desulphurization is occurred at higher temperature.

The weight losses of the Silicalite-1 sample (Figure 8 A, a) due to the degradation of the TPA^+ template are occurred at 345 °C (9 %) and 420 °C (3 %). After removal of the small amount of water below 200°C from MPTS-Silicalite-1 (1 %), a major weight loss at 310 °C (17 %) followed by two peaks at about 440 °C (2.1 %) and 570 °C (5.7 %) were measured. The first step is from sulfur-containing molecules arising from propanethiol decomposition and then propylene is evolved from grafted alkyl chains.

The improved hydrophobicity of the MPTS-modified samples compared to pure silica was further confirmed by kinetics measurements at 85 % RH (Figure 9). It is well-known that Silicalite-1 is hydrophobic in nature as it doesn't contain aluminum. However, depending on the amount of structural defects, Silicalite-1 samples show a certain degree of hydrohilicity as well, and the effect is more pronounced for nanosized Silicalite-1 samples. Colloidal silica, on the other hand, is hydrophilic in nature. Thus, the mass change with time of FD-SiO_2 is larger compared to that of Silicalite-1 (Fig. 9 a, b). The mass gain with time of both MPTS-SiO_2 and MPTS-Silicalite-1 samples was less pronounced in comparison with the mass gain of corresponding non-modified samples. However, the decrease in mass gain was larger for the MPTS-SiO_2 sample (from ca. 8.7% mass change for FD-SiO_2 to ca. 2.2 % for MPTS-SiO_2, Fig. 7 (d)) compared to the decrease for MPTS-Silicalite-1 (from ca. 5.4 % for Silicalite-1 to ca. 3.7 % for MPTS-Silicalite-1, Fig. 7 c). This can be explained by the pore structure of FD-SiO_2 sample making the grafting procedure more efficient.

Textural properties

The porosity of the samples was studied by N_2 adsorption; the measurements were carried out on calcined samples (Fig. 10). All isotherms contain hysteresis loop indicating the presence of mesopores. The hysteresis loop in the pure Silicalite-1 isotherm is related to the presence of mesopores and micropores in the agglomerates of nanosized particles with large external surface area. For the MPTS-Silicalite-1 sample after calcinations the shape of the isotherm changes to a nearly type I characteristic of microporous materials (see Fig. 10 b). Moreover, the nitrogen uptake at low relative pressure (below 0.1 P/P_0) was higher for the MPTS-Silicalite-1 in comparison with Silicalite-1indicating a higher microporosity of the former. The BET surface areas calculated from the range 0.05-0.25 P/P_0 for the Silicalite-1 and MPTS-Silicalite-1 were 416 and 477 m^2/g, respectively (Table 3). The microporous volume for all samples was determined by the α-plot method using a Silica-1000 as a

reference non-porous material. The microporous volumes (V_{mic}) were 0.15 and 0.22 $cm^3\ g^{-1}$ for Silicalite-1 and MPTS-Silicalite-1, respectively. In the case of MPTS-SiO_2, the isotherm was of type IV, and a micropore volume of 0.08 $cm^3\ g^{-1}$ and a BET surface area of 262 $m^2\ g^{-1}$ were determined.

Conclusions

Hydrophobic porous materials have been prepared by co-condensation method using 3-mercaptopropyltrimethoxysilane (MPTS) as organo-functional compound and silica co-source. The incorporation of the organo-functional compounds into the zeolite framework has been proven by the NMR and Raman spectroscopy, and supported by TGA analysis. The presence of MPTS results in the formation of mesopores in the organo-functionalized samples. In addition, the MPTS-modified samples showed increased hydrophobicity according to TGA and water vapor sorption measurements. The method is simple and, compared to other methods for synthesis of hydrophobic zeolites such as the F route is less toxic and interesting for green chemistry applications.

References

1. A. Corma, Chem. Rev. 97 (1997) 2373.
2. A. Taguchi, F. Schüth, Micropor. Mesopor. Mater. 77 (2005) 1.
3. S. E. Bailey, T. J. Olin, R. M. Bricka, D. D. Adrian, Water Res. 33 (1999) 2469.
4. S. Munsch, M. Hartmann, S. Ernst, Chem. Commun. (2001) 1978.
5. M. Kuronen, R. Harjula, J. Jernström, M. Vestenius, J. Lehto, Phys. Chem. Chem. Phys. 2 (2000) 2655.
6. K. Mukhopadhyay, S. Phadtare, V. P. Vinod, A. Kumar, M. Rao, R. V. Chaudhari, M. Sastry, Langmuir 19 (2003) 3858.
7. S. Mandal, D. Roy, R. V. Chaudhari, M. Sastry, Chem. Mater. 16 (2004) 3714.
8. R. Voss, A. Thomas, M. Antonietti, G. A. Ozin, J. Mater. Chem. 15 (2005) 4010.
9. Z. Popović, M. Otter, G. Calzaferri, L. De Cola, Angew. Chem. Int. Ed. 46 (2007) 6188.
10. I. I. Slowing, J. L. Vivero-Escoto, C.-W. Wu, V. S.-Y. Lin, Adv. Drug Delivery Rev. 60 (2008) 1278.
11. F. Hoffmann, M. Cornelius, J. Morell, M. Froba, Angew. Chem., Int. Ed. 45 (2006) 3216.
12. H. Yoshitake, New J. Chem. 29 (2005) 1107.
13. A. P. Wight, M. E. Davis, Chem. Rev. 102 (2002) 3589.
14. J. A. Melero, R. V. Grieken, G. Morales, Chem. Rev. 106 (2006) 3790.
15. K. Möller, T. Bein, Chem. Mater. 10 (1998) 2950.
16. J. Liu, X. Feng, G. E. Fryxell, L. Q. Wang, A. Y. Kim, M. Gong, Adv. Mater. 10 (1998) 161.
17. A. Stein, B. J. Melde, R. C. Schroden, Adv. Mater. 12 (2000) 1403.
18. A. Sayari, S. Hamoudi, Chem. Mater. 13 (2001) 3151.
19. S. Huh, J. W. Wiench, J.-C. Yoo, M. Pruski, V. S.-Y. Lin, Chem. Mater. 15 (2003) 4247.
20. B.-Z. Zhan, M. A. White, M. Lumsden, Langmuir 19 (2003) 4205.
21. S. Huber, G. Calzaferri, Angew. Chem. 116 (2004) 6906.
22. H.-X. Li, M. A. Camblor, M. E. Davis, Micropor. Mater. 3 (1994) 117.
23. L. W. Beck, P. Lu, W. P. Weber, M. E. Davis, Micropor Mater. 12 (1997) 361.
24. M. Choi, H. S. Cho, R. Srivastava, C. Venkatesan, D.-H. Choi, R. Ryoo, Nature Mater. 5 (2006) 718.
25. M. Choi, R. Srivastava, R. Ryoo, Chem. Commun. (2006) 4380.
26. R. Srivastava, N. Iwasa, S. Fujita, M. Arai, Chem. Eur. J. 14 (2008) 9507.

27. D. P. Serrano, J. Aguado, J. M. Escola, J. M. Rodriguez, A. Peral, J. Mater. Chem. 18 (2008) 4210.
28. J. Aguado, D. P. Serrano, J. M. Rodríguez, Micropor. Mesopor. Mater. 115 (2008) 504.
29. K. Yamamoto, Y. Sakata, Y. Nohara, Y. Takahashi, T. Tatsumi, Science 300 (2003) 470.
30. K. Yamamoto, Y. Nohara, Y. Domon, Y. Takahashi, Y. Sakata, J. Plevert, T. Tatsumi, Chem. Mater. 17 (2005) 3919.
31. C. W. Jones, K. Tsuji, M. E. Davis, Nature 393 (1998) 52.
32. K. Tsuji, C. W. Jones, M. E. Davis, Micropor. Mesopor. Mater. 29 (1999) 339.
33. C. W. Jones, K. Tsuji, M. E. Davis, Micropor. Mesopor. Mater. 33 (1999) 223.
34. M. El Roz, L. Lakiss, . Valtchev, S. Mintova, F. Thibault-Starzyk Micropor. Mesopor. Mater. 158 (2012) 148.
35. C. W. Jones, M. Tsapatsis, T. Okubo, M. E. Davis, Micropor. Mesopor. Mater. 42 (2001) 21.
36. D. Massiot, F. Fayon, M. Capron, I. King, S. Le Calvé, B. Alonso, J.-O. Durand, B. Bujoli, Z. Gan, G. Hoatson, Magn. Reson. Chem. 40 (2002) 70.
37. X. Feng, G. E. Fryxell, L.-Q. Wang, A. Y. Kim, J. Liu, K. M. Kemer, Science 276 (1997) 923.
38. M. H. Lim, C. F. Blanford, A. Stein, Chem. Mater. 10 (1998) 467.
39. G. Boxhoorn, R. A. van Santen, W. A. van Erp, G. A. Hays, R. Huis, D. Clague, J. Chem. Soc. Chem. Commun. (1982) 264.
40. M. Kovalakova, B. H. Wouters, P. J. Grobet, Micropor. Mesopor. Mater. 22 (1998) 193.
41. M. H. Lim, C. F. Blanford, A. Stein, Chem. Mater. 10 (1998) 467.
42. Q. Yang, M. P. Kapoor, N. Shirokura, M. Ohashi, S. Inagaki, J. N. Kondo, K. Domen, J. Mater. Chem. 15 (2005) 666.
43. F.-Y. Yeoh, A. Matsumoto, Y. Iwase, T. Baba, Catal. Today 132 (2008) 46.
44. H.-M. Kao, L.-P. Lee, A. Palani, Anal. Chem. 80 (2008) 3016.
45. W.-H. Zhang, X. Zhang, L. Zhang, F. Schroeder, P. Harish, S. Hermes, J. Shi, R. A. Fischer, J. Mater. Chem. 17 (2007) 4320.
46. Y.-S. Li, Y. Wang, T. Tran, A. Perkins, Spectrochim. Acta, Part A 61 (2005) 3032.
47. H. Okabayashi, K. Izawa, T. Yamamoto, H. Masuda, E. Nishio, C. J. O'Connor, Colloid Polym. Sci. 280 (2002) 135.
48. I. Diaz, C. Marquez-Alvarez, F. Mohino, J. Perez-Pariente, J. Catal. 193 (2000) 283.
49. I. Diaz, F. Mohino, J. Perez-Pariente, E. Sastre, Thermochimica Acta 413 (2003) 201.

Tables.

Table 1. Chemical composition of as synthesized samples.

Sample	**Elemental analysis**				**TPAOH** (N)	**MPTS** (S)
	g $g(SiO_2)^{-1}$				mmol $g(SiO_2)^{-1}$	
	Si	C	N	S		
FD SiO2						
	0.467	nd	nd	nd		
MPTS-SiO_2						
	0.467	0.154	nd	0.061	-	1.9
Silicalite-1						
	0.467	0.109	0.013	nd	0.9	-
MPTS-Silicalite-1						
	0.467	0.37	0.013	0.13	0.9	4.1

nd = non detected

Table 2. TG/DTG data of as-synthesized samples.

Sample	Temperature (°C) and weight loss (%)					Total weight loss at 800°C (%)
MPTS-SiO_2	200°C	260°C	320°C	380°C	520°C	15.1
	1.1%	1.5%	5.5%	7%		
Silicalite-1	200°C		345°C	420°C		15.5
	3.5%		9%	3%		
MPTS-Silicalite-1	200°C		310°C	440°C	560°C	26.4
	1%		17%	2.1%	5.7%	

Table 3. Textural properties of calcined samples determined by N_2 sorption measurements.

Sample	V_{total} (cm^3 g^{-1})	V_{mic} (cm^3 g^{-1})	S_{BET} (m^2 g^{-1})
FD-SiO_2	0.241	0.003	209
MPTS-SiO_2	0.208	0.080	262
Silicalite-1	0.422	0.153	416
MPTS-Silicalite-1 (calcined)	0.271	0.221	477
MPTS-Silicalite-1 (plasma)	0.273	0.150	379

V_{total} is determined at $P/P_0 = 0.99$

V_{mic} is determined from α-plot

S_{BET} is determined from the P/P_0 range (0.05 – 0.25)

Figures

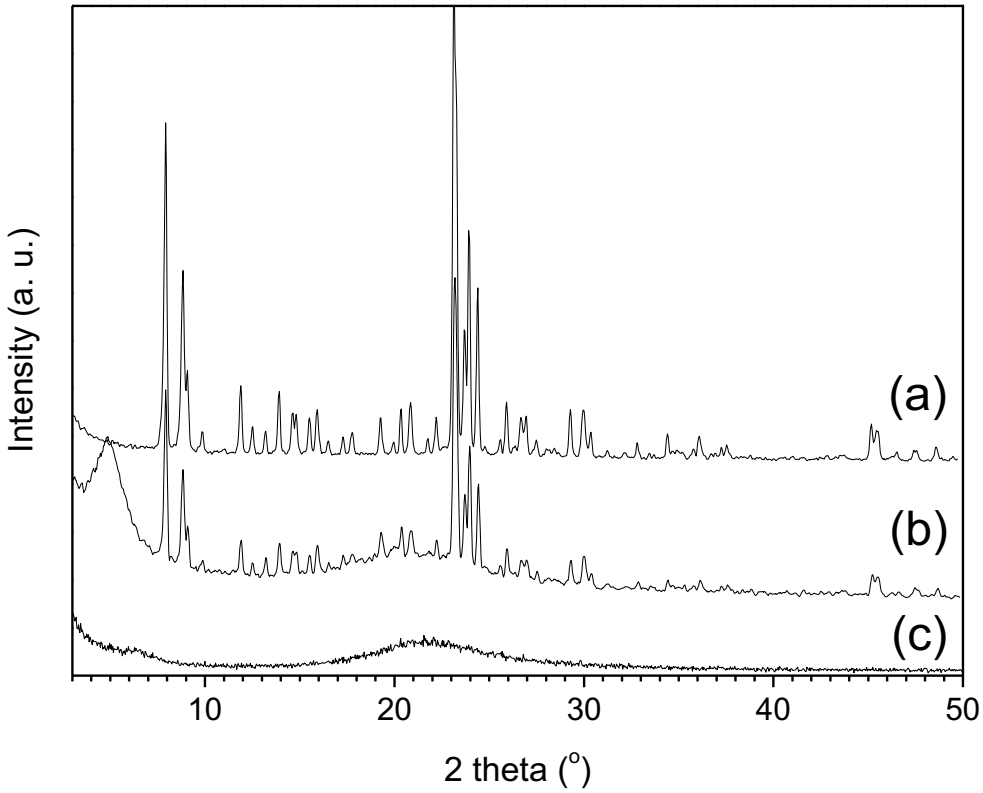

Figure 1. XRD patterns of (a) Silicalite-1, (b) MPTS-Silicalite-1, and (c) MPTS-SiO_2.

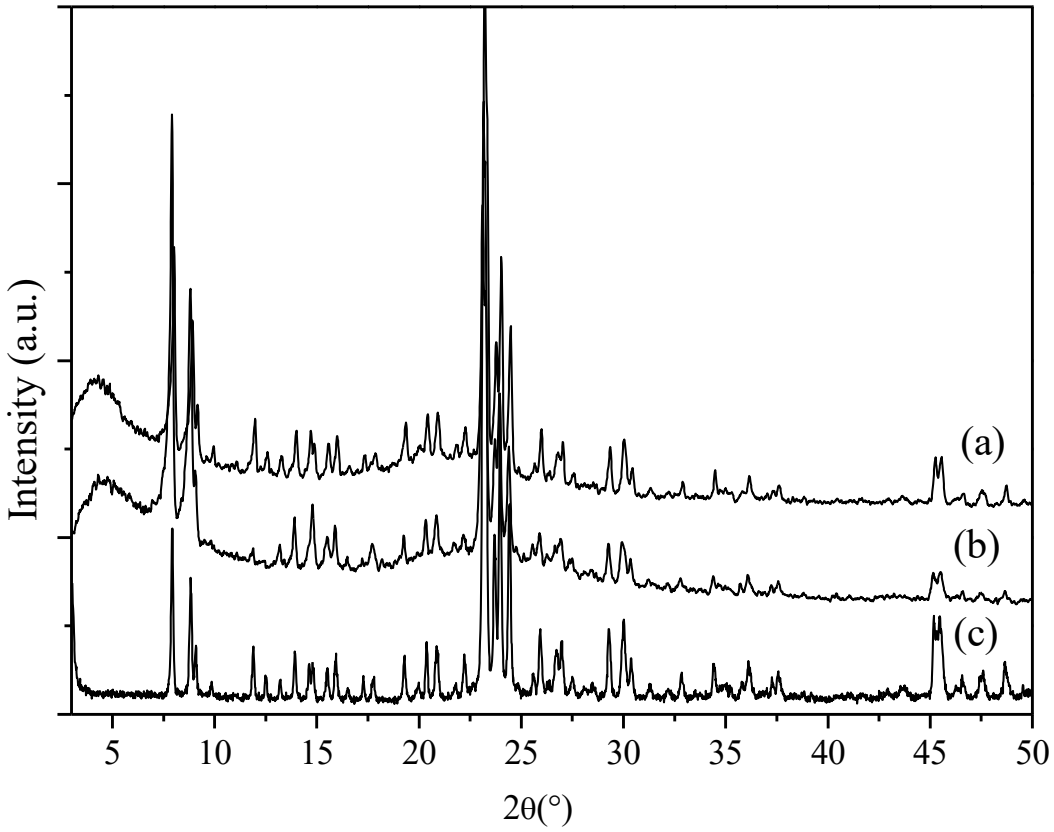

Figure 2. XRD patterns of the MPTS-Silicalite-1 (a) as-prepared, (b) plasma treated and (c) after calcination.

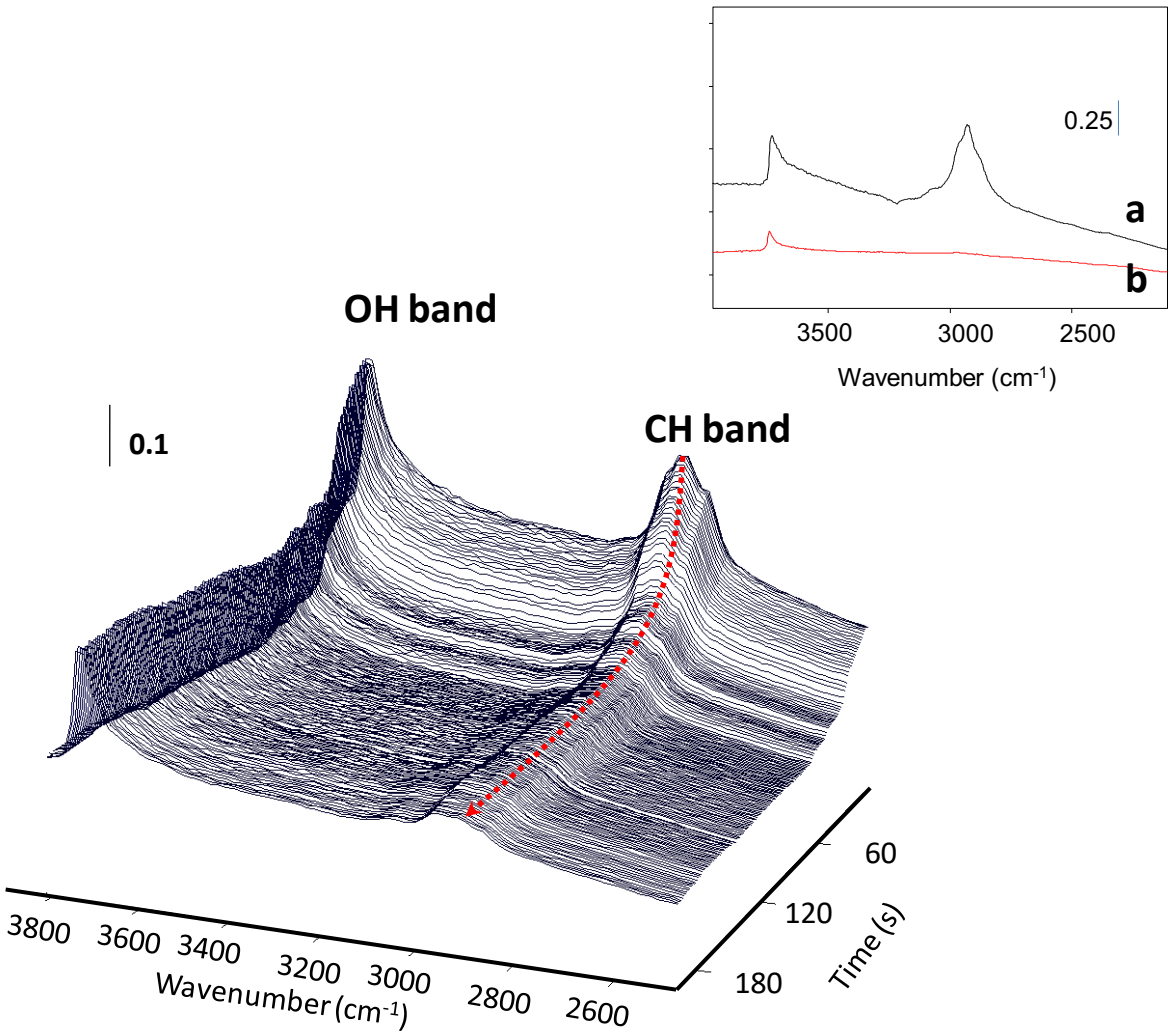

Figure 3. Evolution of IR spectrum of MPTS-Silicalite-1 sample during O_2-plasma treatment. *Insert:* IR spectra collected for the sample after 1 min (a) and 10 min (b) of O_2-plasma treatment.

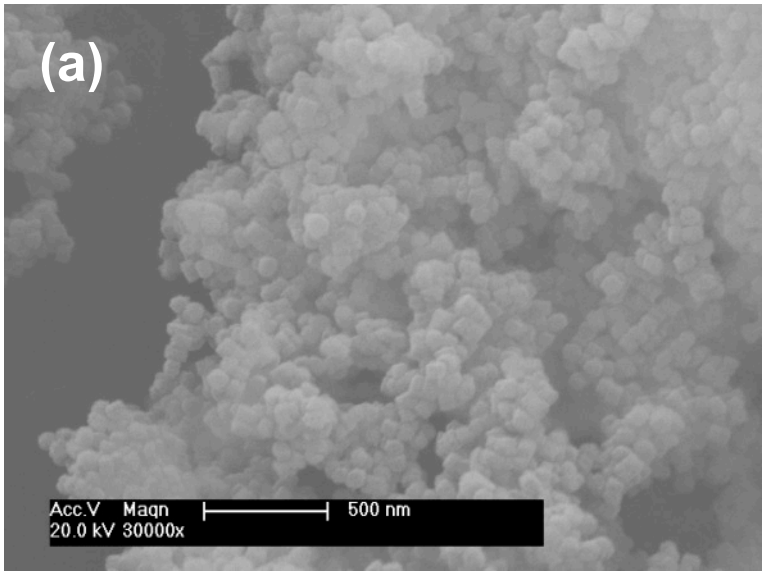
(a)
Acc.V Magn
20.0 kV 30000x
500 nm

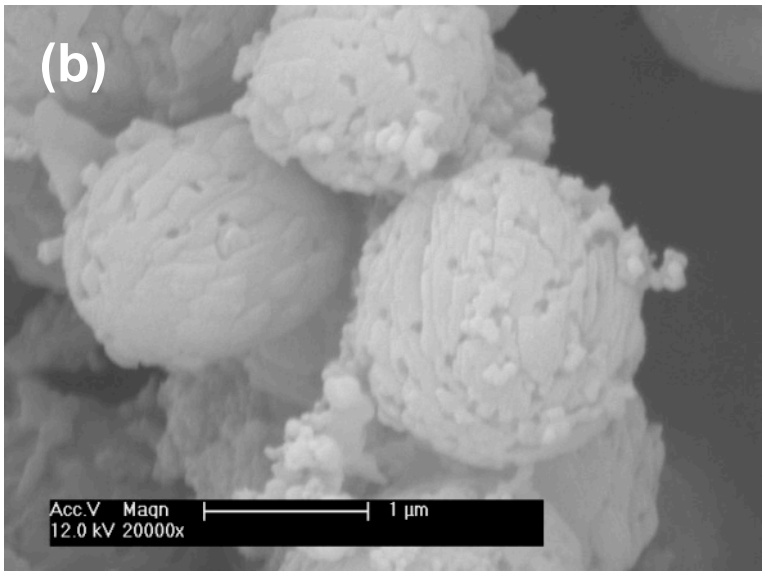
(b)
Acc.V Magn
12.0 kV 20000x
1 µm

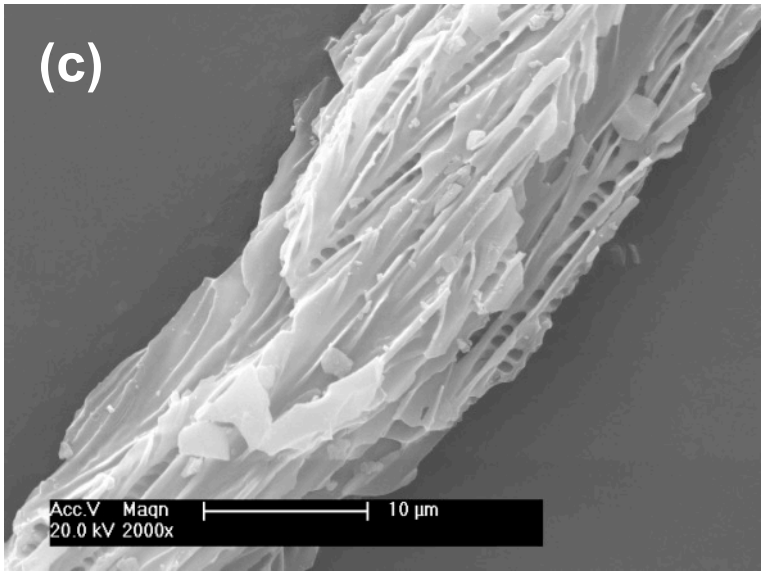

Figure 4. SEM images of (a) Silicalite-1, (b) MPTS-Silicalite-1, and (c) MPTS-SiO_2.

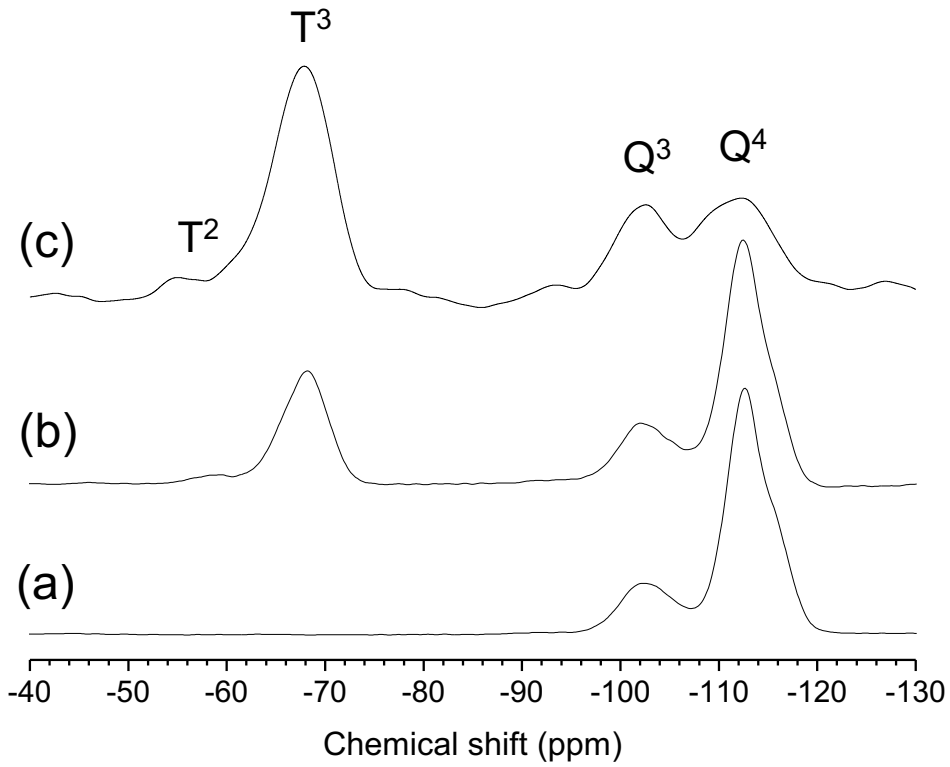

Figure 5. ^{29}Si CP-MAS NMR spectra of (a) Silicalite-1, (b) MPTS-Silicalite-1, and (c) MPTS-SiO_2.

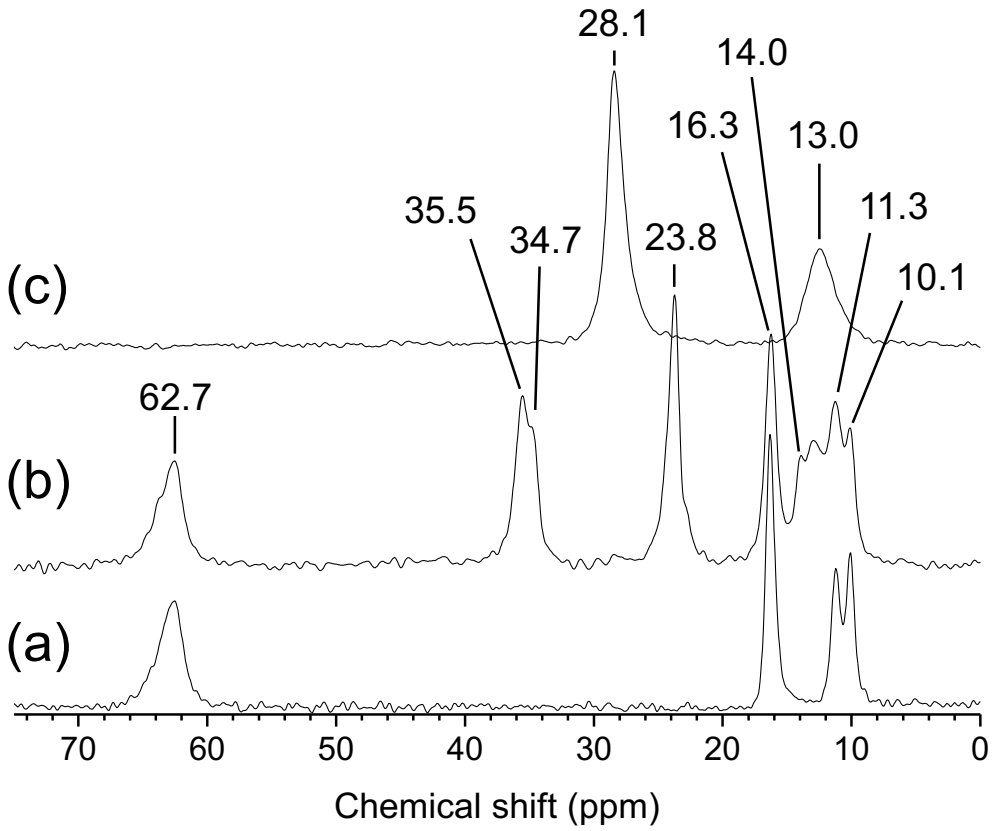

Figure 6. ^{13}C CP-MAS NMR spectra of (a) Silicalite-1, (b) MPTS-Silicalite-1, and (c) MPTS-SiO_2.

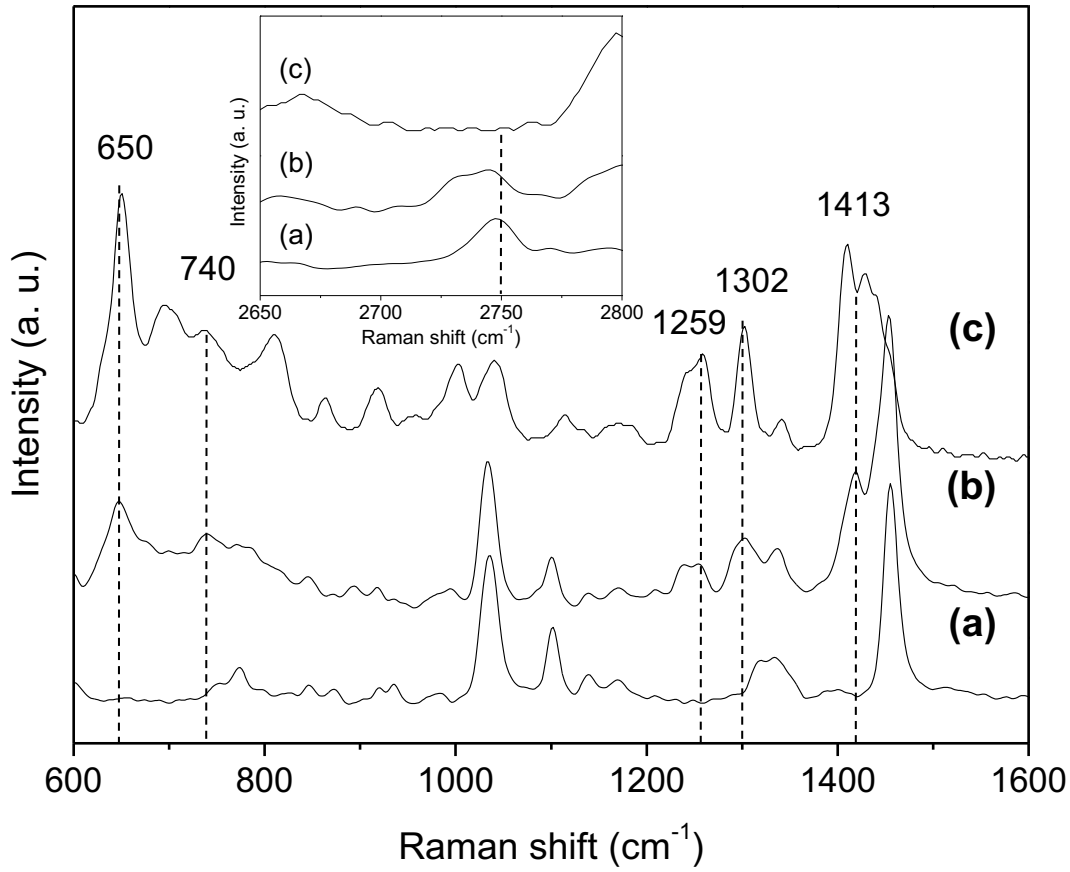

Figure 7. Raman spectra of (a) Silicalite-1, (b) MPTS-Silicalite-1, and (c) MPTS-SiO_2.

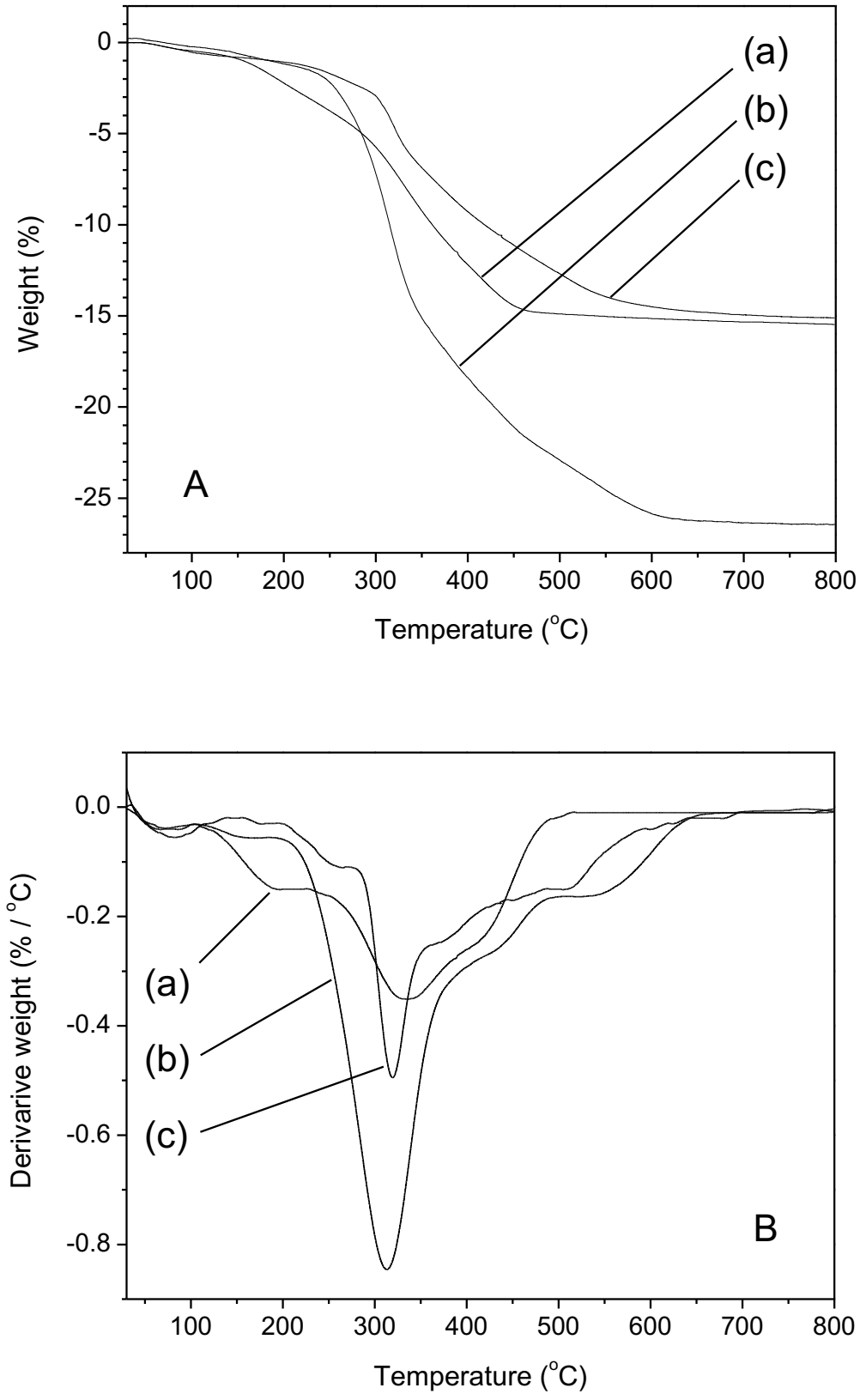

Figure 8. A) TG and B) DTG curves of (a) Silicalite-1, (b) MPTS-Silicalite-1, and (c) MPTS-SiO_2.

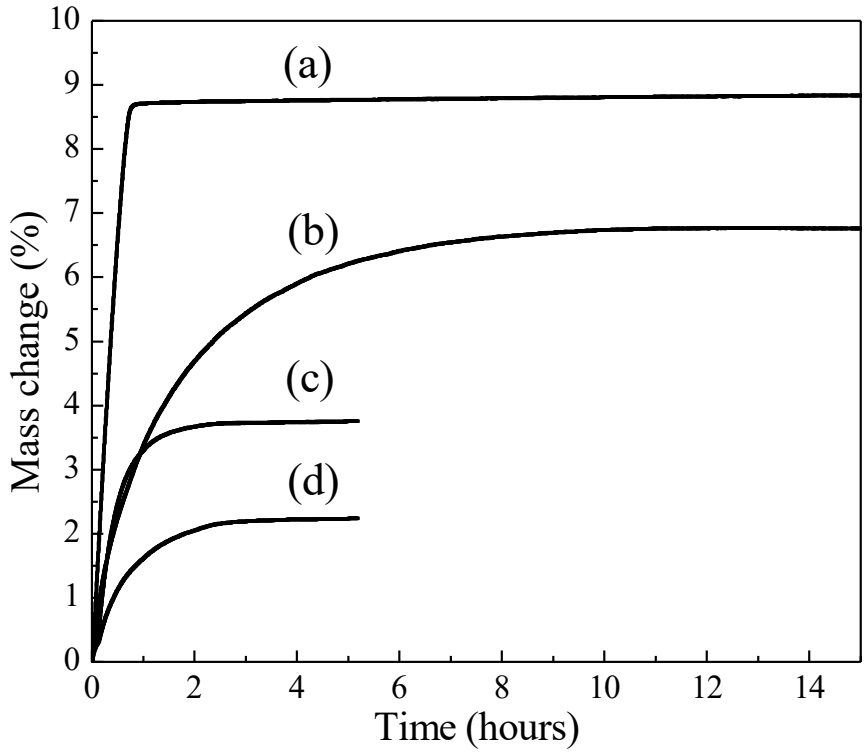

Figure 9. Mass change with time of samples exposed to 85% RH at 25°C: (a) FD-SiO_2, (b) Silicalite-1, (c) MPTS-Silicalite-1 and (d) MPTS-SiO_2.

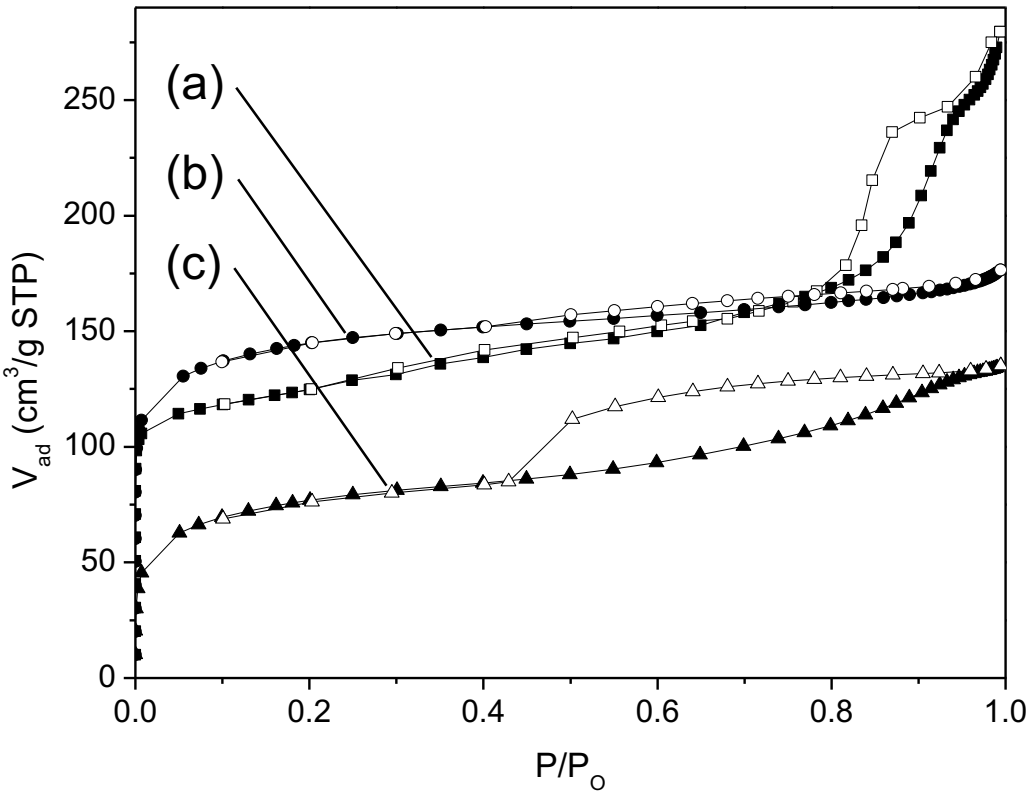

Figure 10 Nitrogen isotherms of (a) TPA-Silicalite-1, (b) MPTS-Silicalite-1 (calcined), (c) MPTS-Silicalite-1 (plasma) and (c) MPTS-SiO_2.!!!!

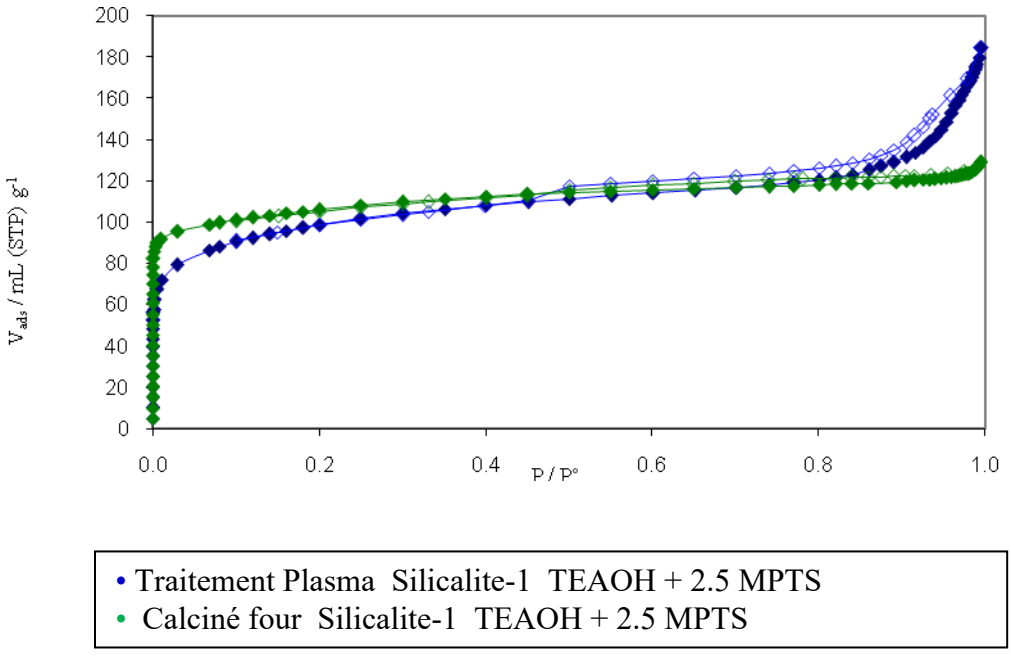

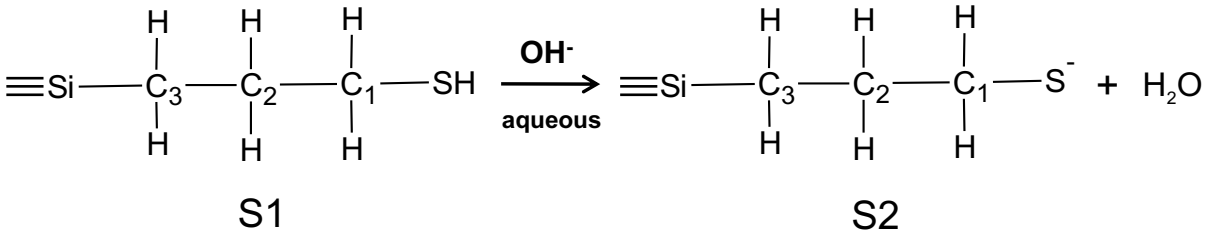

S1 S2

Scheme 1 Deprotonation of 3-mercaptopropyltrimethoxysilane in aqueous base.

Porous materials prepared by co-condensation synthesis approach

Ka-Lun Wong,[†] Mohamad ElRoz,[†] Lubomira Tosheva,[‡] Jean-Michel Goupil,[†] and Svetlana Mintova[†,*]

Hydrophobic porous materials have been prepared by co-condensation method using 3-mercaptopropyltrimethoxysilane (MPTS) as organo-functional compound and silica co-source. The MPTS incorporated into the zeolite framework led to an increased hydrophobicity and formation of mesopores.